A Manganese-Rich Environment Supports Superoxide Dismutase Activity in a Lyme Disease Pathogen, *Borrelia burgdorferi*

J. Dafhne Aguirre[1], Hillary M. Clark[1], Matthew McIlvin[2], Christine Vazquez[1], Shaina L. Palmere[1], Dennis Grab[3], J. Seshu[4], P. John Hart[5], Mak Saito[2] and Valeria C. Culotta[1]

[1]Department of Biochemistry and Molecular Biology, Johns Hopkins University Bloomberg School of Public Health, Baltimore, MD 21205; [2] Marine Chemistry & Geochemistry, Woods Hole Oceanographic Institution, Woods Hole, MA 02543; [3]Department of Pathology, Division of Medical Microbiology, Johns Hopkins University School of Medicine, Baltimore MD 21205; [4]Department of Biology, U. Texas, San Antonio, TX 78249; [5]Department of Veterans Affairs, Geriatric Research, Education and Clinical Center, South Texas Veterans Health Care System, San Antonio, TX, and Department of Biochemistry, University of Texas Health Science Center, San Antonio, TX 78229

Running title: *Manganese and SOD in the Lyme disease pathogen*

To whom correspondence should be addressed: Valeria C. Culotta, Department of Biochemistry and Molecular Biology, Johns Hopkins University Bloomberg School of Public Health, Baltimore, MD 21205, Tel: (410) 955-3029; FAX (410) 955-2926; Email: vculotta@jhsph.edu

Keywords: Lyme disease; manganese; iron; superoxide dismutase; mitochondria

Background: SodA is an important virulence factor in *Borrelia burgdorferi.*
Results: This SodA requires extraordinarily high intracellular manganese for activity, and accumulates as either manganese or apoprotein, but not iron-bound.
Conclusion: *B. burgdorferi* SodA is a unique Mn-SOD based on metal requirements and predicted structure.
Significance: *B. burgdorferi* pathogenicity may be controlled by exploiting the unusual properties of SodA.

SUMMARY

The Lyme disease pathogen *Borrelia burgdorferi* represents a novel organism in which to study metalloprotein biology in that this spirochete has uniquely evolved with no requirement for iron. Not only is iron low, but we show here that *B. burgdorferi* has the capacity to accumulate remarkably high levels of manganese. This high manganese is necessary to activate the SodA superoxide dismutase (SOD) essential for virulence. Using a metalloproteomic approach, we demonstrate that a bulk of *B. burgdorferi* SodA directly associates with manganese and a smaller pool of inactive enzyme accumulates as apoprotein. Other metalloproteins may have similarly adapted to using manganese as co-factor including the BB0366 amino-peptidase. While *B. burgdorferi* SodA has evolved in a manganese-rich, iron-poor environment, the opposite is true for Mn-SODs of organisms such as *E. coli* and bakers' yeast. These Mn-SODs still capture manganese in an iron-rich cell, and we tested whether the same is true for *Borrelia* SodA. When expressed in the iron-rich mitochondria of *S. cerevisiae, B. burgdorferi* SodA was inactive. Activity was only possible when cells accumulated extremely high levels of manganese that exceeded cellular iron. Moreover, there was no evidence for iron inactivation of the SOD. *B. burgdorferi* SodA shows strong overall homology with other members of the Mn-SOD family, but computer assisted modeling revealed some unusual features of the hydrogen bonding network near the enzyme's active site. The unique properties of *B. burgdorferi* SodA may represent adaptation to expression in the manganese-rich and iron-poor environment of the spirochete.

INTRODUCTION

Superoxide dismutases (SOD) represent families of metal-containing enzymes that catalyze the disproportionation of superoxide to hydrogen peroxide and oxygen. One family includes the

Mn- and Fe-SOD enzymes that are well conserved from archaea to humans (1,2). The manganese versus iron binding forms of this family are highly homologous to one another and can bind either metal with similar geometries and metal binding affinities (3-7). Yet Mn-SODs are only active with manganese bound, and substitution with iron in the active site will destroy catalytic activity, largely due to disruption of redox potential. The converse is true with Fe-SODs: manganese binding inactivates the enzyme (8,9). It is therefore critical that these SODs only capture their correct co-factor.

Most organisms are "iron-philic" and accumulate high micromolar to near millimolar levels of iron to catalyze a variety biochemical processes (10-12). Iron accumulation is typically one to two orders of magnitude higher than manganese, and based on the Irving-Williams series, is predicted to bind preferentially to cellular ligands over manganese, placing manganese at an apparent disadvantage for co-factor selection in SODs. Nevertheless, Mn-SOD enzymes have evolved methods for avoiding iron and inserting manganese into the active site, a classic example being the mitochondrial manganese Sod2p of *S. cerevisiae.* In spite of the 50-fold abundance of mitochondrial iron over manganese, Sod2p captures manganese and is virtually impervious to iron inactivation except under rare cases of manganese starvation or with certain yeast mutants of mitochondrial iron overload (1,13,14). Such exclusion of cellular iron appears conserved, as the Mn-SodA from *E. coli* targeted to yeast mitochondria also acquires manganese over the more abundant metal, iron (14).

The need to avoid iron may be obviated with SOD enzymes from the Lyme disease pathogen, *Borrelia burgdorferi*. Elegant studies by Posey and Gherardini have shown that this spirochete fails to accumulate any appreciable iron and does not express any known iron- specific enzymes. The total lack of an iron requirement is advantageous to *B. burgdorferi* during infection when the host attempts to starve pathogens of iron (15-17). *B. burgdorferi* expresses a single SOD of the Fe/Mn family that is essential for virulence (18). Based on the apparent lack of cellular iron, *B. burgdorferi* SodA is proposed to bind manganese (18), yet direct binding of manganese to *B. burgdorferi* SodA has not been demonstrated. Two independent studies have investigated the co-factor specificity of *B. burgdorferi* SodA based on differential H_2O_2 resistance (Mn-SOD enzymes should be resistant to peroxide), but the findings have been conflicting: one report concludes the SOD binds iron (19), whereas a more recent study by Troxell and colleagues concludes *B. burgdorferi* SodA is a Mn-SOD (20). Furthermore, the implications for a SOD enzyme evolving in an iron-deplete cell have not been examined. Can a SOD enzyme that has only seen manganese still capture its co-factor in an iron-rich cellular environment?

Here we investigate the activity and metal requirement for *B. burgdorferi* SodA expressed in its native host versus a heterologous iron-philic host, namely the bakers' yeast *S. cerevisiae*. We find that *B. burgdorferi* can accumulate remarkably high levels of manganese that are needed to support activity of its SodA. Using a metalloproteomic approach, we demonstrate that *B. burgdorferi* SodA exists as active Mn-SOD enzyme as well as inactive apoprotein, but does not bind other metals. When expressed heterologously in the iron-philic host *S. cerevisiae*, *B. burgdorferi* SodA is only active when the yeast accumulates vast quantities of manganese that exceed total cellular iron, a condition analogous to the natural *B. burgdorferi* host. Unlike the homologous Mn-Sod enzymes from yeast and *E. coli*, *B. burgdorferi* SodA does not appear to have evolved with the capacity for capturing manganese in an iron-rich environment.

EXPERIMENTAL PROCEDURES

Strains, growth media and plasmids The *B. burgdorferi* WT strains ML23 and 297 and the *bmtA* mutant were previously described (18,21). All yeast strains were derived from BY4741 and include the isogenic *sod1*Δ*::kanMX4*, *sod2*Δ*::kanMX4* and the *sod1*Δ *sod2*Δ mutant AR142 (22). *E. coli* strain DH5alpha was used.

B. burgdorferi was typically grown in BSK medium (pH 7.6) supplemented with 6% (v/v) rabbit serum (Sigma) also containing 0.05mg/ml rifampicin, 0.1mg/ml phosphomycin, and 5ug/ml amphotericin b (18). BSK medium supplemented with synthetic Ex-cyte (Millipore) rather than rabbit serum was prepared precisely as described (15). *B. burgdorferi* cultures were

typically inoculated from frozen stocks at a density of $10^4$and grown at 34°C (unless indicated otherwise) to a density of $10^8 – 10^9$ cells/ml. Yeast strains were grown in an enriched YPD at 30°C (yeast extract, peptone, dextrose) and *E. coli* was grown in BSK medium without antibiotics and at 37°C.

The pAN002 plasmid for expressing *E. coli* SodA in the mitochondria of yeast and under the yeast *SOD2* promoter and terminator was previously described (14). Plasmid pDA002 is a derivative of pAN002 in which the SodA coding region of *E. coli* was replaced with *B. burgdorferi* SodA. A DNA cassette was synthesized (Celtek Genes) consisting of the open reading frame of *B. burgdorferi* SodA that was codon-optimized for expression in yeast and engineered to contain flanking NdeI and BglII restriction sites at the start and stop codons respectively. The cassette was inserted into the pGH vector (Celtek Genes) and following digestion with NdeI and BglII, the mobilized cassette was introduced into plasmid pAN002 digested with these same enzymes, replacing the *E. coli SodA* coding region with *B. burgdorferi SodA*. In the resultant plasmid pDA002, *B. burgdorferi* SodA was fused in-frame to the mitochondrial leader sequence (MLS) of *S. cerevisiae* Sod2p and under the *SOD2* gene promoter. Plasmid pSP002 for expressing *B. burgdorferi* SodA in the yeast cytosol was constructed by removing the MLS in plasmid pDA002. A NdeI site was introduced by oligo-directed mutagenesis at the yeast *SOD2* start site for translation. Digestion with NdeI and re-ligation resulted in removal of the MLS. All plasmids were verified by DNA sequencing.

Biochemical analyses For preparation of *B. burgdorferi* cell lysates, cultures of *B. burgdorferi* were inoculated at a density of 10^4 cells/ml and grown to 3-8 x10^7 cells/ml. Cells were harvested by centrifugation at 3200xg at 4°C, and washed twice in PBS and twice in metal free deionized water prior to resuspension in lysis buffer containing 10mM sodium phosphate pH 7.8, 5 mM EDTA, 5 mM EGTA, 50 mM NaCl, 0.45% (v/v) NP40. Cells were lysed in a TissueLyser using 0.7 mm zirconium oxide beads (3 cycles at 50Hz for 3 min interspersed with 3 min on ice). Lysates were then clarified by centrifugation at 20,000xg for 10 min at 4°C. To prepare lysates for native and denaturing gel analyses, 45 ml cultures were used and cells were lysed in 150 µl lysis buffer also containing 10% (v/v) glycerol. For large-scale lysate preparations as required for multi-dimensional chromatography (see below), 600 ml cultures were used, and cells were lysed in 2.0 mls buffer lacking glycerol. *E. coli* lysates for metal analysis were prepared as described above for *B. burgdorferi*, using *E. coli* grown in BSK medium at 37°C to OD_{600} ≈2.0. *S. cerevisiae* lysates were prepared from strains grown non-shaking for 20 hrs in YPD medium to a final OD_{600} of ≈1.0 – 5.0. Cells were lysed by glass bead homogenization as described (23), except the lysis buffer also contained 10% (v/v) glycerol. In all cases, protein concentration was determined by Bradford.

For measurements of SOD protein and activity, lysates from *S. cerevisiae* or *B. burgdorferi* were partially enriched for SODs by heating at 42°C for 20 min followed by centrifugation at 20,000xg. This treatment removes ≈30% of total cellular protein with no loss in activity or protein levels of Cu/Zn SODs or the Mn SodAs of *B. burgdorferi* or *E. coli*. SOD activity was carried by the native gel assay (14,24). Lysates from *B. burgdorferi* (2.5 – 25 µg cellular protein) or from *S. cerevisiae* (50-75 µg) were subjected to native gel electrophoresis using 12% precast gels (Invitrogen) and staining with nitroblue tetrazolium (NBT) as described (14,24). For *in-gel* inactivation of SODs by peroxide, gels were soaked in 50 mM phosphate buffer pH 8.1 containing the designated concentrations of H_2O_2 for 1 hour prior to rinsing in H_2O and incubating in NBT staining solution. To specifically inactivate yeast Cu/Zn Sod1p, 5 mM H_2O_2 was used. For immunoblot analyses, 0.5 – 10.0 µg of *B. burgdorferi* or 50-75 µg *S. cerevisiae* lysate protein was subject to denaturing gel electrophoresis on 10% polyacrylamide SDS–gels, followed by transfer to membranes and hybridization to a mouse anti-SodA antibody (18) at 1:1500 - 2000 dilution and a secondary donkey anti-mouse antibody at 1:5000. Where indicated, *S. cerevisiae* blots were also probed with an anti-yeast Sod2p (14) and Pgk1p (23) antibodies as described.

For whole cell manganese analysis of *B. burgdorferi* by atomic absorption spectroscopy (AAS) ≈10^9 cells grown and harvested as

described above were washed twice in either PBS or TE (10 mM Tris 1 mM EDTA, pH 7.6) (results were identical with either PBS or TE), followed by dual washes in metal free milliQ water. Cells were resuspended in 1 ml 65-70% (v/v) nitric acid (Ultrex, high purity) and heated at 80°C for 1 hr. Cell debris was removed by centrifugation for 5 minutes at 20,000xg. Samples were diluted 1:14 (WT) or 1:2 (*bmtA* mutant) in metal free milliQ H_2O prior to analysis by graphite furnace AAS (Perkin Elmer Analyst 600). AAS measurements of manganese in soluble protein lysates used lysates from *B. burgdorferi*, *S. cerevisiae* and *E. coli* prepared as described above.

For iron and manganese analysis by Inductively coupled plasma mass spectrometry (ICP-MS), $10^9 - 10^{10}$ *B. burgdorferi* cells grown and harvested as above were washed twice in TE and once in metal free milliQ water. As a blank control, the same volume of BSK medium incubated in parallel but with no cells was subjected to the identical centrifugation and washing treatments. The no cell control and *B. burgdorferi* pellet were heated in nitric acid and clarified by centrifugation as described above for AAS. Samples were diluted 1:30 in metal free milliQ H_2O and analyzed by ICP-MS (Agilent 7500ce; Johns Hopkins NIEHS Center Core facility). Any elements detected in the blank control were subtracted from the *B. burgdorferi* sample. Under these conditions, there was no iron that could be detected above background in *B. burgdorferi*. ICP-MS analyses of whole yeast cells and *E. coli* were carried out in the same manner using 10^8 *S. cerevisiae* cells grown in YPD or 10^8 *E. coli* cells grown in BSK.

Multi-dimensional chromatography for metal analysis of B. burgdorferi SodA.

Soluble *B. burgdorferi* lysates were diluted in TRIS buffer (50 mM, pH=8.8) and loaded onto an anion exchange column (1 mL HP HiTrap Q, GE Healthcare Life Sciences) at 0.5 mL/min. Proteins were eluted with 0.1, 0.2, 0.3, 0.4, 0.5, and 1 M sodium chloride TRIS buffer (50 mM, pH=8.8) solutions. The 0.3 and 0.4 M NaCl elutions were concentrated using 3000 MWCO spin columns (VIVASPIN 500, Sartorius Stedim Biotech) then injected onto a size exclusion column (0.5 mL/min, 10 mM TRIS buffer, 50 mM NaCl, pH=7.5, TSKgel G3000SWXL, TOSOH Bioscience) with fractions collected each minute. Aliquots of each eluted fraction were prepared for proteomic and ICP-MS mass spectrometry analyses. Proteomic samples were digested with trypsin (Trypsin Gold, Promega Corp.). For elemental analysis by ICP-MS each fraction aliquot was diluted 1:4 into 5% (v/v) nitric acid containing 1ppb In as an internal standard. ICP-MS analysis was performed on a Thermo Element 2 with an Aridus spray chamber (CETAC Technologies) with external calibration by plasma standards (SPEX CertiPrep Ltd.) and correction for matrix effects by In normalization.

LC/MS samples were concentrated onto a peptide cap trap and rinsed with 150uL 0.1% formic acid and 5% acetonitrile (v/v) in water, before gradient elution through a reversed phase Magic C18 AQ column (0.1 x 150 mm, 3 μm particle size, 200 Å pore size, Michrom Bioresources Inc.) on an Advance HPLC system (Michrom Bioresources Inc.) at a flow rate of 500 nL/min. The chromatography consisted of a gradient from 5% buffer A to 95% buffer B for 80 min, where A was 0.1% formic acid in water and B was 0.1% formic acid in acetonitrile. A LTQ linear ion trap mass spectrometer (Thermo Scientific Inc.) was used with an ADVANCE CaptiveSpray source (Michrom Bioresources Inc.). The LTQ was set to perform MS/MS on the top 5 ions using data-dependent settings, and ions were monitored over a range of 400-2000 m/z. Protein identifications were conducted using SEQUEST (Bioworks Version 3.3, Thermo Inc.) using filters of delta CN >0.1, >30% ions, Xcorr vs charge state of 1.9, 2.4, 2.9 for +1, +2, and +3 charges, respectively, and peptide probability of <1e-3. Protein identifications and relative protein abundances in each fraction (as normalized spectral counts) were also determined using Scaffold using protein and peptide probability settings of 99.9% and 95% and two tryptic peptides, respectively (Proteome Software, Version 3.5.1).

RESULTS

Activity of SodA in its native B. burgdorferi host

B. burgdorferi can be cultured outside the host in the laboratory using a serum-rich "BSK" growth medium. In these conditions, *B. burgdorferi* is

seen to express a single SodA superoxide dismutase whose activity can be detected by a native gel assay (Fig. 1A and (18-20). To test whether SodA expression was dependent on serum factors, we replaced the 6% rabbit serum with Ex-cyte, a synthetic substitute (15). As seen in Fig. 1A, there is no change in SodA protein levels or enzymatic activity in cells cultured with synthetic Ex-cyte supplements, indicating activity is not dependent on serum protein factors. We also examined effects of variations in growth conditions that have been reported to mimic the environment of the tick host, namely growth at pH 7.6, 23^{o}C and at pH 6.7, 37^{o}C, to simulate the unfed and post-blood meal conditions, respectively (25). As seen in Fig. 1B, *B. burgdorferi* SodA protein levels and activity are maximal under the laboratory conditions thought to best simulate the post-blood meal state.

Direct association of manganese with B. burgdorferi SodA

Based on the virtual absence of iron in *B. burgdorferi*, SodA is most likely a manganese enzyme, and this notion has been supported by recent studies examining peroxide resistance of the SOD (20). As seen in Fig. 1C, *B. burgdorferi* SodA follows the H_2O_2 resistance of the mitochondrial Mn Sod2p of bakers' yeast (Fig. 1C, far right panel). However, peroxide resistance is not definitive proof of manganese binding, as Fe-SOD enzymes can also be characterized as somewhat peroxide-resistant. As seen in Fig. 1C, both Fe- and Mn-SODs retain activity with mM levels of H_2O_2 that inactivate Cu/Zn Sod1p. Hence, more direct methods of metal analysis are required. To this end, we carried out a metalloproteomic approach (26-30) to identifying the co-factor associated with *B. burgdorferi* SodA.

Soluble *B. burgdorferi* lysates were resolved by two-dimensional (strong anion exchange and size exclusion) chromatography under non-denaturing conditions (31) and fractionated proteins were digested with trypsin and identified by reversed-phase LC/MS and linear trap MS. Figure 2 shows results from resolution of the 300 and 400 mM ion exchange fractions found to contain the SodA polypeptide. The peak of SodA protein identified by mass spectrometry in fractions 18,19 (Fig. 2A top) retained full enzymatic activity (Fig. 2B); hence the SOD retained its metal co-factor during fractionation. A shoulder of SodA protein eluting in fraction 20 (Fig. 2A top) was devoid of enzymatic activity (Fig. 2B) and may be missing metal co-factor. Indeed by ICP-MS, there is a well-defined manganese peak that co-eluted with active SodA in fractions 18 and 19, but not with inactive SodA in fraction 20; moreover, there was no clear association between SodA and iron (Fig. 2A, B). Likewise, zinc and copper failed to associate with the SodA protein (not shown). SodA was the only protein that closely overlapped this manganese peak. While there was a partial overlap with a fructose bis aldolase and EF-2 translation initiation factor in fraction 18, this could not account for the manganese signal in fraction 19 (Fig. 2A, C). Together these results demonstrating a tight association between active SodA enzyme and manganese (but not iron) establish SodA as a manganese-dependent SOD.

It is noteworthy that in addition to the SodA-containing peak in manganese, there was a second manganese peak eluting earlier by size exclusion (Fig. 2A). This second peak completely overlaps with a *B. burgdorferi* aminopeptidase (BB0366) that, in various organisms, uses iron, zinc, or manganese as a co-factor (32-35). This study underscores the power of multi-dimensional chromatography coupled to quantitative proteomics in identification of metal-protein partnerships.

SodA is active in a manganese-rich, iron-free host

Posey and Gheridini have reported that *B. burgdorferi* is virtually free of cellular iron (15), and we have confirmed these findings using ICP-MS (Fig. 3A). In the course of these metal analyses, we noted the spirochete accumulates unusually high levels of manganese. As seen in Fig. 3A, *B. burgdorferi* accumulated two orders of magnitude higher levels of manganese per cell than *E. coli* grown in BSK medium in parallel. This high level of manganese was seen with both the ML23 and the 297 strain backgrounds and by metal analysis with both AAS and ICP-MS (Fig. 3A and 3C). Because cell volumes for the spirochete are difficult to estimate, we normalized manganese on the basis of soluble cellular protein and compared values in *B. burgdorferi*, *E. coli* and the eukaryote, bakers' yeast. Yeast and *E. coli* are reported to accumulate similar µM concentrations

of manganese (10,11), and we also find similar manganese levels in these organisms when analyzed per mg protein (Fig. 3B). By comparison, the level of manganese that accumulated in *B. burgdorferi* was two orders of magnitude higher (Fig. 3B).

The exceptionally high level of manganese in *B. burgdorferi* is required for maximal SodA activity. When the manganese transporter BmtA is deleted in *B. burgdorferi*, there is a one to two orders of magnitude drop in cellular manganese (21) to levels within the range of WT *E. coli* (Fig. 3C top). This drop in manganese results in inactive SodA (Fig. 3D top). Unlike previous findings by Troxell and colleagues (20), we observe no change in *B. burgdorferi* SodA protein levels with this loss in enzymatic activity. Hence high manganese is required to activate the enzyme and not regulate expression of SodA. We also addressed the effects of raising intracellular manganese on *B. burgdorferi* SodA activity. Manganese levels can double by growing *B. burgdorferi* in the presence of 10 μM $MnCl_2$ (severe toxicity ensues above this) (Fig. 3C bottom), but this rise in manganese does not increase the enzymatic activity nor protein levels of *B. burgdorferi* SodA (Fig. 3D bottom). The enzyme appears maximally activated in the manganese rich environment of *B. burgdorferi* without additional metal supplements.

Expression of B. burgdorferi SodA in an iron-philic host: S. cerevisiae

Manganese containing SOD enzymes are fairly well-conserved in evolution (2), as illustrated in the alignment of MnSODs from *B. burgdorferi, E. coli* and yeast (Fig. 4A). Yet unlike *B. burgdorferi*, the environment of *E. coli* and yeast would seem hostile to activation of a Mn-SOD enzyme. These organisms are iron-philic and accumulate intracellular levels of iron that far exceed manganese (10,36). Can a SOD that evolved in a manganese rich environment acquire its co-factor in an iron rich host? To address this, we expressed SodA in the mitochondria of *S. cerevisiae* where manganese activation of SOD enzymes has been well characterized (13,14,37,38).

B. burgdorferi SodA codon-optimized for expression in yeast was fused to the mitochondrial leader sequence (MLS) of yeast Sod2p (indicated in Fig. 4A) and placed under control of the yeast *SOD2* promoter. Expression of SodA was first analyzed in the background of a *sod1*Δ yeast to avoid interference from yeast Cu/Zn Sod1p that migrates to similar positions on the native gel for SOD activity (see Fig. 1C). As seen in Fig. 4B, *sod1*Δ cells co-expressing the endogenous yeast Sod2p and *B. burgdorferi* SodA in the mitochondria only exhibited activity of the endogenous yeast Mn Sod2p (lane 7). However, *B. burgdorferi* SodA activity was gained with high levels of manganese (lanes 9-12) that were toxic to yeast as indicated by growth inhibition (Fig. 4B bottom). This dependence on high manganese for SodA activity was not due to oxidative damage from expression in the *sod1* null strain, as similar results were obtained in WT yeast where Cu/Zn SOD activity on the native gel was eliminated by peroxide treatment (Fig. 5A). Moreover, the yeast mitochondrial Sod2p does not compete with *B. burgdorferi* SodA for manganese, as *B. burgdorferi* SodA activity was not increased in *sod2*Δ null mutants (Fig. 5A, middle panel). *B. burgdorferi* SodA exhibits 46% identity with the SodA from *E. coli* (Fig. 4A), yet *E. coli* SodA driven by the same yeast *SOD2* promoter and MLS is not similarly dependent on toxic manganese for activity (Fig. 5B) as was previously published (14). Thus, the requirement for high manganese is not a general feature of bacterial Mn-SOD enzymes. In the case of *B. burgdorferi* SodA, high manganese is also needed for protein expression (Fig. 5C middle). This is not a transcriptional effect because yeast Sod2p driven by the same *SOD2* promoter remains constant with manganese (Fig. 5C bottom). Instead, manganese activation of *B. burgdorferi* SodA seems to stabilize the protein expressed in yeast mitochondria.

We also tested the effects of expressing *B. burgdorferi* SodA in the cytosol of *S. cerevisiae* by deleting the MLS for targeting to the mitochondria. As seen in seen Fig. 6, *B. burgdorferi* SodA in the cytosol exhibited the same dependence on high manganese for protein expression and enzymatic activity as was seen with mitochondrial-expressed SodA. Identical results were obtained with expression in a WT strain and in a yeast *sod1*Δ mutant where *B. burgdorferi* SodA represents the sole SOD enzyme of yeast cytosol (Fig. 6).

We sought to determine the level of intracellular manganese required to activate the heterologous *B. burgdorferi* SodA in yeast. Both mitochondrial and cytosolic- expressed *B. burgdorferi* SodA require roughly 500 μM extracellular manganese to detect any activity, and this reflects a 50-100-fold increase in intracellular accumulation of manganese (Fig. 7A). Interestingly, treatment with high manganese also results in a drastic reduction in cellular iron levels (Fig. 7A), perhaps due to competing effects of manganese on iron uptake.

We tested whether the loss in cellular iron seen with high manganese contributes to the activation of *B. burgdorferi* SodA in yeast. Iron levels in yeast cells can be lowered by treatment with the iron chelator, bathophenanthroline disulfonate (BPS) (14), and as seen in Fig. 7A, BPS effectively lowered cellular iron levels by 25-fold without changes in intracellular manganese. This lowering of iron was sufficient to induce activity of a yeast Mn-SOD expressed in yeast cytosol and also increased activity of mitochondrial yeast Sod2p (Fig 7B) consistent with the notion that a certain pool of yeast Sod2p is iron-bound inactive enzyme (13,14). It is noteworthy that the cytosolic version of *S. cerevisiae* Sod2p is more strongly activated by manganese than by BPS compared to endogenous mitochondrial Sod2p (Fig. 7B). Apparently in the cytosol where manganese is limiting, iron depletion on its own cannot maximally activate *S. cerevisiae* Sod2p. Although BPS was effective in increasing activity of yeast Sod2p, it failed to activate the *B. burgdorferi* SodA enzyme or stabilize the SodA polypeptide expressed in either the cytosol (Fig. 7B, bottom; Fig. 7C, lane 2) or in the mitochondria of yeast (Fig. 7C, compare lanes 5 and 6). BPS also did not enhance the effects of high manganese in activating *B. burgdorferi* SodA (Fig. 7C, compare lanes 3 and 4, and lanes 7 and 8). Therefore, lowering cellular iron is by itself insufficient to activate *B. burgdorferi* SodA and high levels of manganese are essential. It is noteworthy that the high manganese:iron ratio required to activate *B. burgdorferi* SodA in yeast is not unlike the situation in the native *B. burgdorferi* host, where manganese levels are exceedingly high and iron is virtually absent.

DISCUSSION

B. burgdorferi has uniquely evolved without a cellular requirement for iron, and we show here that the organism accumulates high levels of manganese compared to other more iron-philic organisms such as *E. coli* and *S. cerevisiae*. This environment of high manganese and a virtual absence of iron is well-suited for activation of a manganese SodA. Through a metalloproteomic approach, we firmly establish SodA as a manganese enzyme and show that in *Borrelia*, the active enzyme is bound to manganese while a smaller pool of inactive enzyme is apo, not bound to any other metal. By comparison, the Mn-SODs from other organisms such as yeast, *E. coli* and human can bind intracellular iron (5,6,39-41). We have no evidence for iron binding to *B. burgdorferi* SodA in either its native spirochete host or in the iron-rich environment of yeast mitochondria. In addition, *B. burgdorferi* SodA activity requires exceedingly high levels of intracellular manganese. When expressed in *S. cerevisiae*, the enzyme is only active when manganese levels exceed mitochondrial iron, conditions that simulate the native *B. burgdorferi* host.

The accumulation of unusually high manganese in *B. burgdorferi* that we report here has not been previously documented, although our values are very similar to those published by Ouyang et al (21). In studies by Posey and Gherardini, the manganese in *B. burgdorferi* cell lysates was reported to be only 2-3-fold higher than that of *E. coli* (15) and might reflect differential growth conditions used, as our cells were grown to near stationary phase. In any case, our findings clearly demonstrate a tremendous capacity for manganese uptake without toxicity in this spirochete. In fact, in our preliminary studies comparing manganese across various species (not shown), the levels of the metal in whole cell *B. burgdorferi* are comparable to *L. plantarum*, notoriously known for hyper-accumulating manganese, without a SOD enzyme (42).

The high manganese in *B. burgdorferi* may serve dual purposes in the adaptation of this pathogen. First, in the absence of iron-requiring enzymes, manganese may be more widely used as a co-factor. Consistent with this, we observe a close association with *B. burgdorferi* manganese

and an aminopeptidase (Fig. 2A), a metalloenzyme that employs iron in other organisms (35). Moreover, the ability of *B. burgdorferi* to accumulate high manganese may represent yet another fascinating adaptation of the organism to the metal starvation response of innate immunity. When infected, the host not only systemically starves pathogens of iron (16,17), but macrophages and neutrophils attempt to limit manganese bioavailability for the invading species (43-45). High manganese is essential for virulence in *B. burgdorferi* (21) and SodA may only be part of the story. Non-proteinaceous complexes of manganese to small metabolites (so-called Mn-antioxidants) are receiving increasing attention as critical factors in microbial oxidative stress resistance and pathogenesis (1,46-51).

Very recently, Wang et. al have reported iron accumulation in *B. burgdorferi* (52). This report appears in direct conflict with the previous findings of Posey and Gherardini (15) and with our ICP-MS analysis of iron. The basis for the iron reported by Wang et al. cannot be reconciled at this time but might reflect the differential extraction methods used for metal analysis. Alternatively, under certain non-standard laboratory conditions, the bacteria may be capable of iron uptake.

Lastly, why does *B. burgdorferi* SodA require such high levels of cellular manganese for activity? Currently there are no structural data available on *B. burgdorferi* SodA, however, we were able to generate a computer assisted model of *B. burgdorferi* SodA using MODELLER (53) based on known structures of *E. coli* SodA and *S. cerevisiae* Sod2p. A comparison of the active site regions of *E. coli* and *B. burgdorferi* SodA molecules is shown in Fig. 8A. The manganese coordination site is identical between the two SODs, however several interesting features emerge. For example, the second sphere residue F34 in *B. burgdorferi* SodA is a tyrosine in Mn-SOD molecules ranging from bacteria (e.g., *E. coli, D. radiodurans*) to fungi (*S. cerevisiae*), invertebrates (*C. elegans, D. melanogaster*) and mammals (Fig. 8B). Y34 is well-known is participate in a hydrogen bonding network at the active site (simulated in Fig. 8A), and in fact the Y34F derivatives of human and yeast Mn-SOD have been analyzed in detail and shown to dramatically alter the kinetics of the SOD reaction, disrupting the "prompt protonation pathway" (54-56). However, there were no reports of Y34F affecting manganese binding in human and yeast Mn-SOD. Thus, the unique F34 in *B. burgdorferi* SodA may well account for some enzyme catalysis effects, but not the requirement for high manganese. A second noteworthy residue in *B. burgdorferi* SodA is Y84 which is a phenylalanine in other Mn-SOD enzymes (Fig. 8B). As seen in Fig. 8A, the model predicts that Y84 forms nearly an ideal hydrogen bond with Y181 which could potentially occlude access of manganese to the active site. Such an occlusion would be consistent with the conformationally gated metal uptake mechanism proposed for Mn-SOD molecules (57). However, we observed that the single Y84F substitution in *B. burgdorferi* SodA did not alter the requirement for high manganese (data not shown), indicating that other residues of *B. burgdorferi* SodA must be involved. Our structural model will provide a useful guide in unraveling the unique properties of the enzyme that force its requirement for high manganese *in vivo*.

REFERENCES

1. Aguirre, J. D., and Culotta, V. C. (2012) Battles with iron: manganese in oxidative stress protection. *J. Biol. Chem.* **287**, 13541-13548
2. Wintjens, R., Noel, C., May, A. C., Gerbod, D., Dufernez, F., Capron, M., Viscogliosi, E., and Rooman, M. (2004) Specificity and phenetic relationships of iron- and manganese-containing superoxide dismutases on the basis of structure and sequence comparisons. *J. Biol. Chem.* **279**, 9248-9254
3. Mizuno, K., Whittaker, M. M., Bachinger, H. P., and Whittaker, J. W. (2004) Calorimetric studies on the tight-binding metal interactions of *Escherichia coli* manganese superoxide dismutase. *J. Biol. Chem.* **279**, 27339-27344
4. Iranzo, O. (2011) Manganese complexes displaying superoxide dismutase activity: a balance between different factors. *Bioorg. Chem.* **39**, 73-87
5. Kang, Y., He, Y., Zhao, M., and Li, W. (2011) Structures of native and Fe-substituted SOD2 from Saccharomyces cerevisiae. *Acta Cryst. Sec. F*
6. Yamakura, F., and Kawasaki, H. (2010) Post-translational modifications of superoxide dismutase. *Biochim. Biophys. Acta* **1804**, 318-325
7. Yamakura, F., Kobayashi, K., Furukawa, S., and Suzuki, Y. (2007) In vitro preparation of iron-substituted human manganese superoxide dismutase: possible toxic properties for mitochondria. *Free Radic. Biol. Med.* **43**, 423-430
8. Vance, C. K., and Miller, A. F. (1998) A Simple Proposal That Can Explain the Inactivity of Metal-Substituted Superoxide Dismutases. *J. Am. Chem. Soc.* **120**, 461-467
9. Jackson, T. A., and Brunold, T. C. (2004) Combined spectroscopic/computational studies on Fe- and Mn-dependent superoxide dismutases: insights into second-sphere tuning of active site properties. *Acc. Chem. Res.* **37**, 461-470
10. Outten, C. E., and O'Halloran, T. V. (2001) Femtomolar Sensitivity of Metalloregulatory Proteins Controlling Zinc Homeostasis. *Science* **292**, 2488-2492
11. Rosenfeld, L., Reddi, A. R., Leung, E., Aranda, K., Jensen, L. T., and Culotta, V. C. (2010) The effect of phosphate accumulation on metal ion homeostasis in Saccharomyces cerevisiae. *J. Biol. Inorg. Chem.* **15**, 1051-1062
12. Eide, D. J., Clark, S., Nair, T. M., Gehl, M., Gribskov, M., Guerinot, M. L., and Harper, J. F. (2005) Characterization of the yeast ionome: a genome-wide analysis of nutrient mineral and trace element homeostasis in Saccharomyces cerevisiae. *Genome Biol.* **6**, R77
13. Yang, M., Cobine, P. A., Molik, S., Naranuntarat, A., Lill, R., Winge, D. R., and Culotta, V. C. (2006) The effects of mitochondrial iron homeostasis on cofactor specificity of superoxide dismutase 2. *EMBO J.* **25**, 1775-1783
14. Naranuntarat, A., Jensen, L. T., Pazicni, S., Penner-Hahn, J. E., and Culotta, V. C. (2009) The interaction of mitochondrial iron with manganese superoxide dismutase. *J. Biol. Chem.* **284**, 22633-22640
15. Posey, J. E., and Gherardini, F. C. (2000) Lack of a role for iron in the Lyme disease pathogen. *Science* **288**, 1651-1653
16. Correnti, C., and Strong, R. K. (2012) Mammalian siderophores, siderophore-binding lipocalins, and the labile iron pool. *J. Biol. Chem.* **287**, 13524-13531
17. Johnson, E. E., and Wessling-Resnick, M. (2012) Iron metabolism and the innate immune response to infection. *Microbes Infect.* **14**, 207-216
18. Esteve-Gassent, M. D., Elliott, N. L., and Seshu, J. (2009) sodA is essential for virulence of Borrelia burgdorferi in the murine model of Lyme disease. *Mol. Microbiol.* **71**, 594-612
19. Whitehouse, C. A., Williams, L. R., and Austin, F. E. (1997) Identification of superoxide dismutase activity in Borrelia burgdorferi. *Infect. Immun.* **65**, 4865-4868

20. Troxell, B., Xu, H., and Yang, X. F. (2012) Borrelia burgdorferi, a pathogen that lacks iron, encodes manganese-dependent superoxide dismutase essential for resistance to streptonigrin. *J. Biol. Chem.* **287**, 19284-19293
21. Ouyang, Z., He, M., Oman, T., Yang, X. F., and Norgard, M. V. (2009) A manganese transporter, BB0219 (BmtA), is required for virulence by the Lyme disease spirochete, Borrelia burgdorferi. *Proc. Natl. Acad. Sci. U. S. A.* **106**, 3449-3454
22. Reddi, A. R., and Culotta, V. C. (2011) Regulation of Manganese Antioxidants by Nutrient Sensing Pathways in Saccharomyces cerevisiae. *Genetics* **189**, 1261-1270
23. Gleason, J. E., Corrigan, D. J., Cox, J. E., Reddi, A. R., McGinnis, L. A., and Culotta, V. C. (2011) Analysis of hypoxia and hypoxia-like states through metabolite profiling. *PLoS One* **6**, e24741
24. Flohe, L., and Otting, F. (1984) Superoxide dismutase assays. in *Methods in enzymology: oxygen radicals in biological systems* (Packer, L. ed.), Academic press, New York. pp 93-104
25. Karna, S. L., Sanjuan, E., Esteve-Gassent, M. D., Miller, C. L., Maruskova, M., and Seshu, J. (2011) CsrA modulates levels of lipoproteins and key regulators of gene expression critical for pathogenic mechanisms of Borrelia burgdorferi. *Infect. Immun.* **79**, 732-744
26. Yannone, S. M., Hartung, S., Menon, A. L., Adams, M. W., and Tainer, J. A. (2012) Metals in biology: defining metalloproteomes. *Curr. Opin. Biotechnol.* **23**, 89-95
27. Lancaster, W. A., Praissman, J. L., Poole, F. L., 2nd, Cvetkovic, A., Menon, A. L., Scott, J. W., Jenney, F. E., Jr., Thorgersen, M. P., Kalisiak, E., Apon, J. V., Trauger, S. A., Siuzdak, G., Tainer, J. A., and Adams, M. W. (2011) A computational framework for proteome-wide pursuit and prediction of metalloproteins using ICP-MS and MS/MS data. *BMC Bioinformatics* **12**, 64
28. Cvetkovic, A., Menon, A. L., Thorgersen, M. P., Scott, J. W., Poole, F. L., 2nd, Jenney, F. E., Jr., Lancaster, W. A., Praissman, J. L., Shanmukh, S., Vaccaro, B. J., Trauger, S. A., Kalisiak, E., Apon, J. V., Siuzdak, G., Yannone, S. M., Tainer, J. A., and Adams, M. W. (2010) Microbial metalloproteomes are largely uncharacterized. *Nature* **466**, 779-782
29. Waldron, K. J., Tottey, S., Yanagisawa, S., Dennison, C., and Robinson, N. J. (2007) A periplasmic iron-binding protein contributes toward inward copper supply. *J. Biol. Chem.* **282**, 3837-3846
30. Robinson, N., Waldron, K., Tottey, S., and Bessant, C. (2008) Metalloprotein metal pools: identification and quantification by coupling native and non-native separations through principal component analysis. *Protocal Exchange*
31. Tottey, S., Patterson, C. J., Banci, L., Bertini, I., Felli, I. C., Pavelkova, A., Dainty, S. J., Pernil, R., Waldron, K. J., Foster, A. W., and Robinson, N. J. (2012) Cyanobacterial metallochaperone inhibits deleterious side reactions of copper. *Proc. Natl. Acad. Sci. U .S. A.* **109**, 95-100
32. Gu, Y. Q., Holzer, F. M., and Walling, L. L. (1999) Overexpression, purification and biochemical characterization of the wound-induced leucine aminopeptidase of tomato. *Eur. J. Biochem.* **263**, 726-735
33. Hafkenscheid, J. C., and Kohler, B. E. (1985) A continuous method for the determination of leucine aminopeptidase in human serum with L-leucinamide as substrate. *J. Clin. Chem. Clin. Biochem.* **23**, 393-398
34. Kale, A., Pijning, T., Sonke, T., Dijkstra, B. W., and Thunnissen, A. M. (2010) Crystal structure of the leucine aminopeptidase from Pseudomonas putida reveals the molecular basis for its enantioselectivity and broad substrate specificity. *J. Mol. Biol.* **398**, 703-714
35. Sule, N., Singh, R. K., Zhao, P., and Srivastava, D. K. (2012) Probing the metal ion selectivity in methionine aminopeptidase via changes in the luminescence properties of the enzyme bound europium ion. *J. Inorg. Biochem.* **106**, 84-89

36. Rosenfeld, L., and Culotta, V. C. (2012) Phosphate disruption and metal toxicity in Saccharomyces cerevisiae: Effects of RAD23 and the histone chaperone HPC2. *Biochem. Biophys. Res. Commun.* **418**, 414-419
37. Luk, E., Carroll, M., Baker, M., and Culotta, V. C. (2003) Manganese activation of superoxide dismutase 2 in Saccharomyces cerevisiae requires MTM1, a member of the mitochondrial carrier family. *Proc. Natl. Acad. Sci. USA* **100**, 10353-10357
38. Luk, E., and Culotta, V. C. (2001) Manganese superoxide dismutase in *S. cerevisiae* acquires its metal co-factor through a pathway involving the Nramp metal transproter, Smf2p. *J. Biol. Chem.* **276**, 47556-47562
39. Whittaker, M. M., and Whittaker, J. W. (2012) Metallation state of human manganese superoxide dismutase expressed in Saccharomyces cerevisiae. *Arch Biochem. Biophys.* **523**, 191-197
40. Privalle, C. T., and Fridovich, I. (1992) Transcriptional and maturation effects of manganese and iron on the biosynthesis of manganese-superoxide dismutase in *Escherichia coli*. *J. Biol. Chem.* **267**, 9140-9145
41. Beyer, W. F., and Fridovich, I. (1991) *In vivo* competition between iron and manganese for occupancy of the active site region of the manganese-superoxide dismutase of Escherichia coli. *J. Biol. Chem.* **266**, 303-308
42. Archibald, F. S., and Fridovich., I. (1981) Manganese and defenses against oxygen toxicity in *Lactobacillus plantarum*. *J. Bacteriol.* **145**, 422-451
43. Cassat, J. E., and Skaar, E. P. (2012) Metal ion acquisition in Staphylococcus aureus: overcoming nutritional immunity. *Semin. Immunopathol.* **34**, 215-235
44. Kehl-Fie, T. E., and Skaar, E. P. (2010) Nutritional immunity beyond iron: a role for manganese and zinc. *Curr. Opin. Chem. Biol.* **14**, 218-224
45. Govoni, G., and Gros, P. (1998) Microphage NRAMP1 and its role in resistance to microbial infections. *Inflamm. Res.* **47**, 277-284
46. Horsburgh, M. J., Wharton, S. J., Cox, A. G., Ingham, E., Peacock, S., and Foster, S. J. (2002) MntR modulates expression of the PerR regulon and superoxide resistance in Staphylococcus aureus through control of manganese uptake. *Mol. Microbiol.* **44**, 1269-1286
47. Horsburgh, M. J., Wharton, S. J., Karavolos, M., and Foster, S. J. (2002) Manganese: elemental defence for a life with oxygen. *Trends Microbiol.* **10**, 496-501
48. Seib, K. L., Tseng, H. J., McEwan, A. G., Apicella, M. A., and Jennings, M. P. (2004) Defenses against oxidative stress in Neisseria gonorrhoeae and Neisseria meningitidis: distinctive systems for different lifestyles. *J. Infect. Dis.* **190**, 136-147
49. Tseng, H. J., Srikhanta, Y., McEwan, A. G., and Jennings, M. P. (2001) Accumulation of manganese in Neisseria gonorrhoeae correlates with resistance to oxidative killing by superoxide anion and is independent of superoxide dismutase activity. *Mol. Microbiol.* **40**, 1175-1186
50. Kehl-Fie, T. E., Chitayat, S., Hood, M. I., Damo, S., Restrepo, N., Garcia, C., Munro, K. A., Chazin, W. J., and Skaar, E. P. (2011) Nutrient Metal Sequestration by Calprotectin Inhibits Bacterial Superoxide Defense, Enhancing Neutrophil Killing of Staphylococcus aureus. *Cell Host Microbe* **10**, 158-164
51. Daly, M. J., Gaidamakova, E. K., Matrosova, V. Y., Kiang, J. G., Fukumoto, R., Lee, D. Y., Wehr, N. B., Viteri, G. A., Berlett, B. S., and Levine, R. L. (2010) Small-molecule antioxidant proteome-shields in Deinococcus radiodurans. *PLoS One* **5**, e12570
52. Wang, P., Lutton, A., Olesik, J., Vali, H., and Li, X. (2012) A novel iron- and copper-binding protein in the Lyme disease spirochaete. *Mol. Microbiol.* **86**, 1441-1451
53. Sali, A., and Blundell, T. L. (1993) Comparative protein modelling by satisfaction of spatial restraints. *J. Mol. Biol.* **234**, 779-815

54. Sheng, Y., Butler Gralla, E., Schumacher, M., Cascio, D., Cabelli, D. E., and Selverstone Valentine, J. (2012) Six-coordinate manganese(3+) in catalysis by yeast manganese superoxide dismutase. *Proc. Natl. Acad. Sci. U S A* **109**, 14314-14319
55. Guan, Y., Hickey, M. J., Borgstahl, G. E., Hallewell, R. A., Lepock, J. R., O'Connor, D., Hsieh, Y., Nick, H. S., Silverman, D. N., and Tainer, J. A. (1998) Crystal structure of Y34F mutant human mitochondrial manganese superoxide dismutase and the functional role of tyrosine 34. *Biochemistry* **37**, 4722-4730
56. Perry, J. J., Hearn, A. S., Cabelli, D. E., Nick, H. S., Tainer, J. A., and Silverman, D. N. (2009) Contribution of human manganese superoxide dismutase tyrosine 34 to structure and catalysis. *Biochemistry* **48**, 3417-3424
57. Whittaker, J. W. (2010) Metal uptake by manganese superoxide dismutase. *Biochim. Biophys. Acta* **1804**, 298-307
58. Sikorski, R. S., and Hieter, P. (1989) A system of shuttle vectors and yeast host strains designed for efficient manipulation of DNA in *Saccharomyces ceresiviae*. *Genetics* **122**, 19-27

Acknowledgements We thank Dr. M. Norgard for the bmtA mutant and Jana Mihalic for ICP-MS. This work was supported in part by the JHU NIEHS center and National Institutes of Health Grants R01 ES08996 and GM50016 (to V. C. C.), and SC1 AI078559 (to J. Seshu). Metalloproteomic studies were funded by the Gordon and Betty Moore Foundation Marine Microbiology Program and a National Science Foundation Chemical Oceanography Grant OCE-1031271 (to M.A.S.). P.J.H. is supported by the Robert A. Welch Foundation (AQ-1399) and in part by VA grant I01BX000506, South Texas Veterans Health Care system. HMC is supported by T32 GM080189.

The abbreviations used are: SOD – superoxide dismutase; YPD – yeast extract, peptone, dextrose medium: AAS – atomic absorption spectroscopy; ICP-MS - inductively coupled plasma mass spectrometry; NBT – nitroblue tetrazolium; MLS- mitochondrial leader sequence.

FIGURE LEGENDS

Figure 1: Activity of *B. burgdorferi* SodA in its native host and its sensitivity towards peroxide

(A,B) Whole cell *B. burgdorferi* lysates were prepared from strain ML23 and were analyzed for SOD activity by native gel electrophoresis and NBT staining ("SodA activity") and for SodA protein levels by immunoblot ("SodA protein") as described in *Experimental Procedures*. (A) Cells were grown in BSK medium supplemented with either 6% (v/v) rabbit serum or with the synthetic serum substitute Ex-cyte. Wedge represents increasing levels of lysate protein analyzed: 2.5, 5 and 10 µg for SodA activity and 0.5, 1, and 2.5 µg for immunoblot. (B) Cells were grown in serum containing BSK under the following conditions: "unfed" - pH 7.6, 23^{o}C to simulate unfed tick host (25); "lab" - pH 7.6, 34^{o}C standard laboratory culture conditions; "fed" – pH 6.7, 37^{o}C to simulate post blood meal conditions in the tick host (25). (C) Samples containing the indicated SOD enzymes were subjected to native gel electrophoresis, and prior to staining with NBT for SOD activity, the gel was incubated with the indicated concentrations of H_2O_2 as described in *Experimental Procedures*. "Mn-Sod2p" and "Cu/Zn-Sod1p" represent *S. cerevisiae* SOD enzymes present in 50 µg of total yeast lysate protein. "*B. burgdorferi* SodA" represents 5.0 µg of *B. burgdorferi* lysate protein. "Ec Fe-SodB" = 0.06 units of purified SodB enzyme from *E. coli* (Sigma).

Figure 2: Multi-dimensional chromatography of *B. burgdorferi* lysates:
Soluble *B. burgdorferi* lysates were resolved by anion exchange, and the 300 and 400 mM NaCl elutions were resolved by size exclusion (SE) chromatography; shown are results from fractions 11-22 of increasing retention time on SE. (A) Fractions were subjected to either metal analysis by ICP-MS ("Fe" and "Mn"), where y axis units represent relative abundance; or proteomic analysis by trypsin digestion, LC/MS and MS/MS ("SodA" and "A-peptidase"), where y axis units represent spectral counts. Shaded boxes indicate manganese peak overlaps with SodA and with amino peptidase–1 (gene BB0366). (B) Fractions were analyzed for SodA activity by the native gel assay. (C) Proteomic analysis of fractions to illustrate that the manganese in fraction 19 shows poor correlation with a fructose bisphosphate aldolase ("F-bP aldolase" gene BB0445) and elongation factor EF-2 ("EF-2" gene BB0540).

Figure 3: Metal analysis of *B. burgdorferi* versus iron-philic organisms and effects on SodA activity
(A) ICP MS analysis of manganese and iron was carried out with whole cell *B. burgdorferi* strain ML23 versus *E. coli cells* grown in BSK medium as described in *Experimental Procedures*. (B) AAS measurements of manganese in soluble protein lysates from *B. burgdorferi* strain ML23, *E. coli* and *S. cerevisiae* as described in *Experimental Procedures.* (C) AAS analysis of whole cell manganese in (top) *B. burgdorferi* strain 297 and the corresponding *bmtA* mutant compared to *E. coli* and (bottom) *B. burgdorferi* strain ML23 grown in BSK supplemented with the indicated concentrations of $MnCl_2$. (D) SodA activity and protein levels were examined as in Fig. 1A in (top) *B. burgdorferi* strain 297 and the corresponding *bmtA* mutant and (bottom) *B. burgdorferi* strain ML23 grown with the indicated concentrations of $MnCl_2$.

Figure 4) Targeting *B. burgdorferi* SodA to the mitochondria of *S. cerevisiae*
(A) Alignment of *B. burgdorferi* SodA with the Mn Sod2p of *S. cerevisiae* and the Mn SodA of *E. coli* using CLC sequencer viewer 6.4 software. Asterisks mark identity and dots represent similar residues; red marks metal binding residues. Yellow shaded area marks the unique F34 and Y84 of *B. burgdorferi* SodA (see Fig. 8) and grey shaded area shows the MLS of yeast Sod2p that was fused onto the bacterial SodA genes. (B) A *sod1*Δ yeast strain was transformed where indicated with the pDA002 plasmid for expressing mitochondrial targeted *B. burgdorferi* SodA (lanes 7-12) was grown with the indicated concentrations of $MnCl_2$. *TOP:* SOD activity was monitored by the native gel assay. The position of endogenous yeast Sod2p "Sc Sod2p" and heterologous *B. burgdorferi* SodA are indicated. Mitochondrial Sod2p runs as a doublet or triplet (14) and the same is true for *B. burgdorferi* SodA expressed in yeast mitochondria. *BOTTOM:* Cell growth was monitored turbidimetrically at $OD_{600\ nm}$ and plotted as percentage of control growth obtained in the absence of manganese.

Figure 5: *B. burgdorferi* SodA requires high manganese for activity and expression in yeast mitochondria.
(A) The indicated WT or *sod* mutants of *S. cerevisiae* expressing mitochondrial targeted *B. burgdorferi* SodA were tested for manganese activation of SOD activity and for manganese effects on cell growth (for WT and *sod2*Δ, bottom) as described in Fig. 4 except yeast Cu/Zn Sod1p was inactivated by *in gel* treatment with 5 mM H_2O_2. The position of endogenous yeast Sod2p "Sc Sod2p" and heterologous *B. burgdorferi* SodA on the native activity gels are indicated. (B) The *sod1*Δ *sod2*Δ expressing either empty vector pRS315 (58), or the mitochondrial targeted SodA from either *B. burgdorferi* or *E. coli* on plasmids pDA002 and pAN002 (14) were grown with the indicated concentrations of $MnCl_2$ and analyzed for SOD activity by the native gel assay. The positions of mitochondrial targeted *E. coli* and *B. burgdorferi* SodA are indicated. (C) WT yeast strains expressing mitochondrial *B. burgdorferi* SodA were grown in the presence of the indicated concentrations of $MnCl_2$ and were subjected to

(top) native gel assays for SOD activity as in part A, (middle/bottom) immunoblot (IB) analysis of *B. burgdorferi* SodA and yeast Sod2p protein levels.

Figure 6: Expression of *B. burgdorferi* SodA in yeast cytosol.
The WT yeast strain or *sod1*Δ mutant was transformed with plasmid pSA002 for expressing *B. burgdorferi* SodA in yeast cytosol and cells were cultured with the indicated mM concentrations of $MnCl_2$. (top) SOD activity was assayed as in Fig. 5C. (middle/bottom) Immunoblot (IB) analysis was conducted as in Fig. 5C using antibodies directed against *B. burgdorferi* SodA and yeast cytosolic Pgk1p.

Figure 7: Iron chelation does not help activate *B. burgdorferi* SodA expressed in yeast.
(A) ICP-MS analysis of iron and manganese in whole cells of *S. cerevisiae* grown in the presence of the indicated concentrations of $MnCl_2$ or 100 μM BPS as described in *Experimental Procedures.* (B) Yeast strains transformed with pEL124 (37) for expressing yeast Sod2p in the cytosol (top panel) or with pDA002 for expressing mitochondrial *B. burgdorferi* SodA (bottom panel) were grown in the presence of 1.0 mM $MnCl_2$ (Mn: +) and/or 0.1 mM of the iron chelator BPS (BPS: +) and subjected to SOD activity analysis. (C) Yeast cells expressing either mitochondrial or cytosolic *B. burgdorferi* SodA were treated with manganese or BPS and tested for SOD activity as in part B (top) and for levels of *B. burgdorferi* SodA and *S. cerevisiae* Sod2p by immunoblot as in Fig. 5C (middle, bottom).

Figure 8: The predicted active site of *B. burgdorferi* SodA
(A) A model of *B. burgdorferi* SodA was generated with the program MODELLER (53) using the 0.9 A structure of *E. coli* SodA (PDB accession# 1IX9) as the structural template. Residues of *B. burgdorferi* SodA are in yellow with numbering in red, and the equivalent positions in *E. coli* SodA are marked in green. Red balls indicate water molecules and dotted lines represent hydrogen bonds or the coordination of the manganese ion (aqua ball) to its four amino acid ligands and a single water molecule. (B) A comparison of Tyr 34 and Phe 84 in *B. burgdorferi* SodA with the equivalent positions in Mn SOD molecules from the indicated organisms.

Figure 1

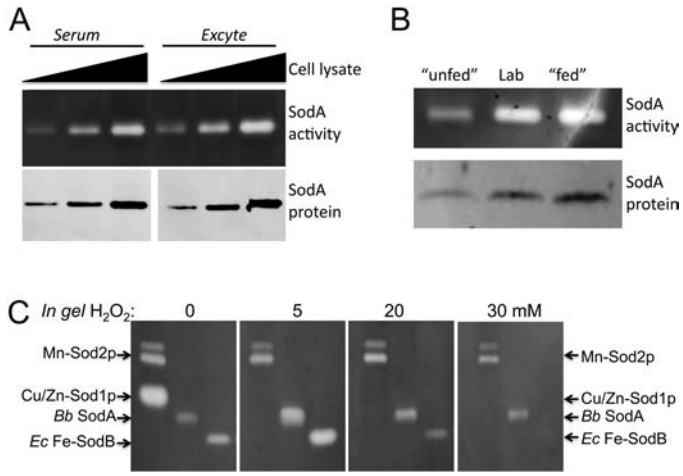
A
Serum
Excyte
Cell lysate
SodA activity
SodA protein
B
"unfed"
Lab
"fed"
SodA activity
SodA protein
C
In gel H2O2:
0
5
20
30 mM
Mn-Sod2p
Cu/Zn-Sod1p
Bb SodA
Ec Fe-SodB

Figure 2

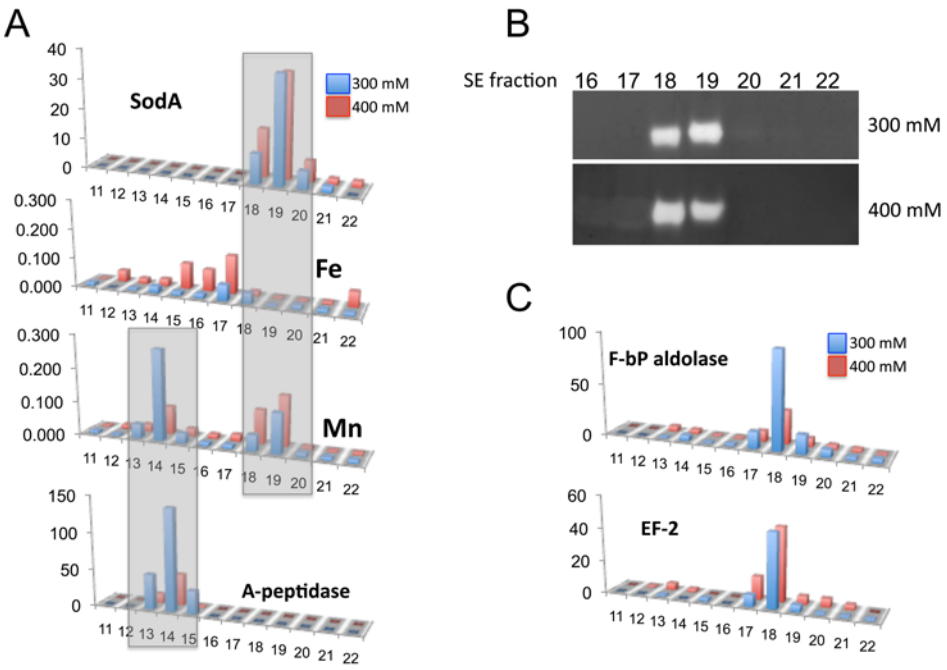
A
SodA
300 mM
400 mM
Fe
Mn
A-peptidase
B
SE fraction 16 17 18 19 20 21 22
300 mM
400 mM
C
F-bP aldolase
300 mM
400 mM
EF-2

Figure 3

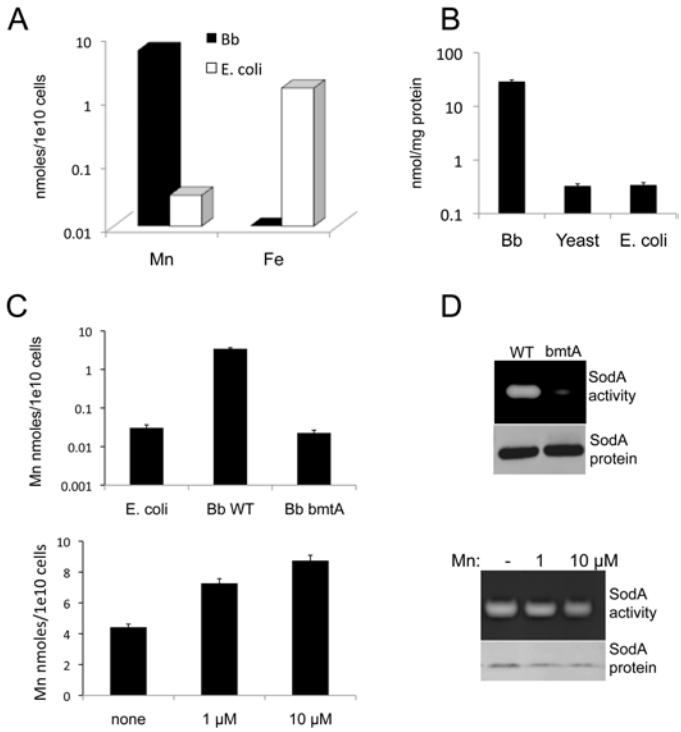
A
Bb
E. coli
nmoles/1e10 cells
10
1
0.1
0.01
Mn
Fe
B
nmol/mg protein
100
10
1
0.1
Bb
Yeast
E. coli
C
Mn nmoles/1e10 cells
10
1
0.1
0.01
0.001
E. coli
Bb WT
Bb bmtA
Mn nmoles/1e10 cells
10
8
6
4
2
0
none
1 μM
10 μM
D
WT
bmtA
SodA activity
SodA protein
Mn:
-
1
10 μM
SodA activity
SodA protein

Figure 4

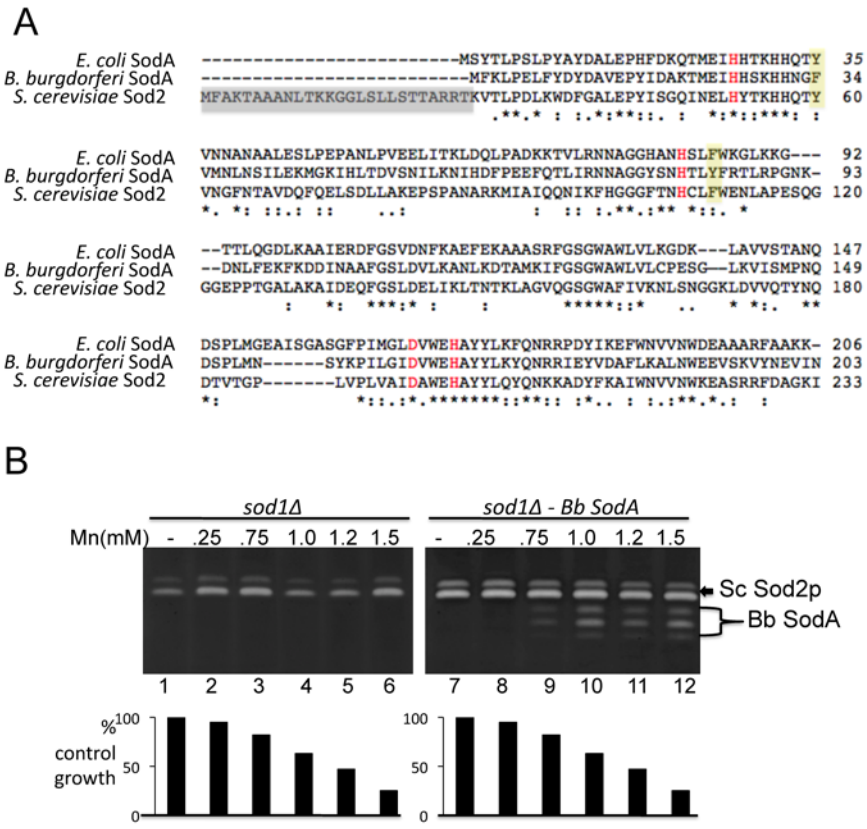
A
E. coli SodA
B. burgdorferi SodA
S. cerevisiae Sod2
B
sod1Δ
sod1Δ - Bb SodA
Mn(mM) - .25 .75 1.0 1.2 1.5
Sc Sod2p
Bb SodA
1 2 3 4 5 6 7 8 9 10 11 12
% control growth
100
50
0

Figure 5

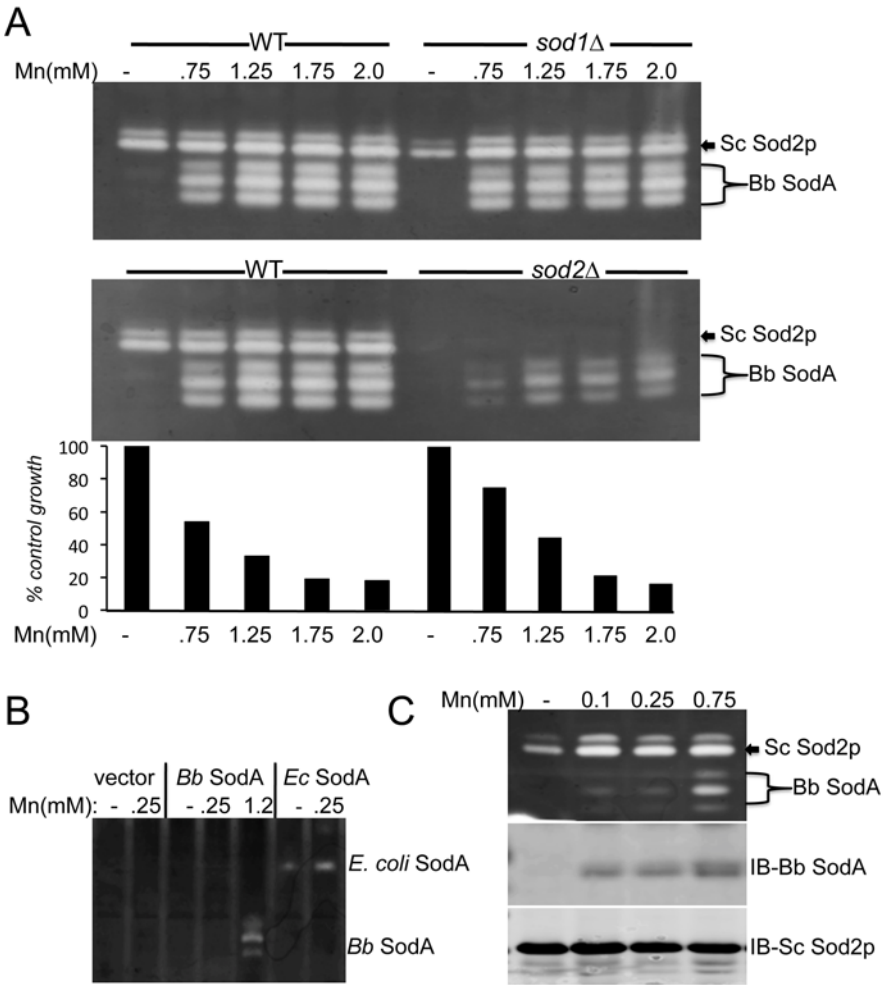
A
WT
sod1Δ
Mn(mM) - .75 1.25 1.75 2.0 - .75 1.25 1.75 2.0
Sc Sod2p
Bb SodA
WT
sod2Δ
Sc Sod2p
Bb SodA
% control growth
100
80
60
40
20
0
Mn(mM) - .75 1.25 1.75 2.0 - .75 1.25 1.75 2.0
B
vector
Bb SodA
Ec SodA
Mn(mM): - .25 - .25 1.2 - .25
E. coli SodA
Bb SodA
C
Mn(mM) - 0.1 0.25 0.75
Sc Sod2p
Bb SodA
IB-Bb SodA
IB-Sc Sod2p

Figure 6

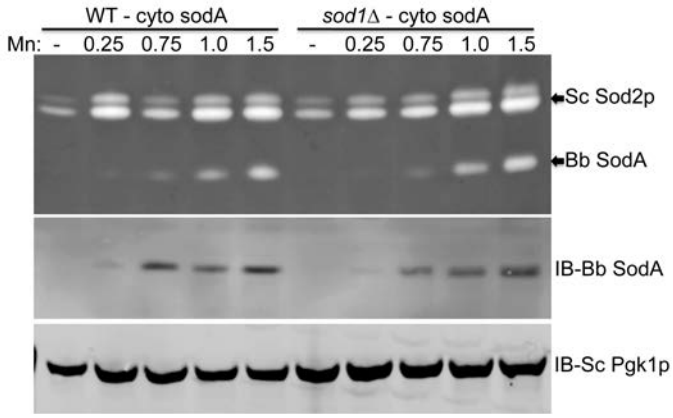
WT - cyto sodA
sod1Δ - cyto sodA
Mn: - 0.25 0.75 1.0 1.5 - 0.25 0.75 1.0 1.5
Sc Sod2p
Bb SodA
IB-Bb SodA
IB-Sc Pgk1p

Figure 7

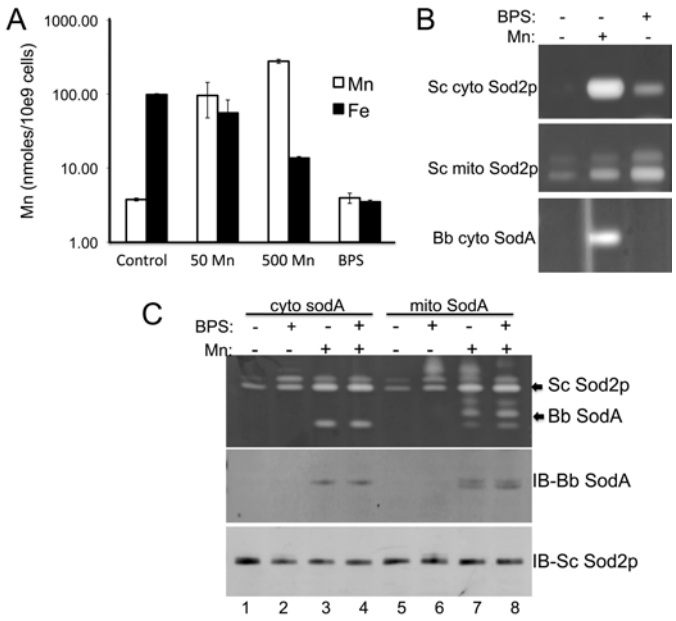
A
1000.00
100.00
10.00
1.00
Mn (nmoles/10e9 cells)
Mn
Fe
Control
50 Mn
500 Mn
BPS
B
BPS: - - +
Mn: - + -
Sc cyto Sod2p
Sc mito Sod2p
Bb cyto SodA
C
cyto sodA
mito SodA
BPS: - + - + - + - +
Mn: - - + + - - + +
Sc Sod2p
Bb SodA
IB-Bb SodA
IB-Sc Sod2p
1 2 3 4 5 6 7 8

Figure 8

A

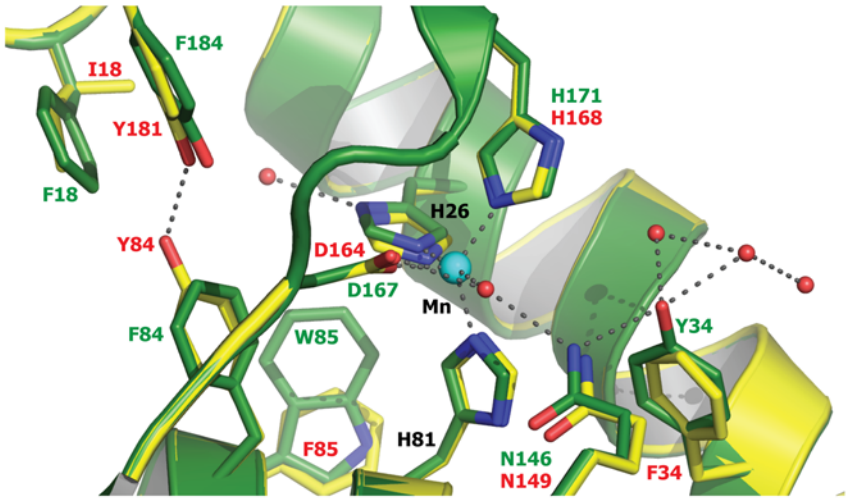

B

H. sapiens	HSKHHAAYVNNLN	GHINHSIFWTNLS
M. musculus	HSKHHAAYVNNLN	GHINHSIFWTNLS
C. elegans	HQKHHATYVNNLN	GHINHSIFWTNLA
D. melanogaster	HQKHHQTYVNNLN	GHINHTIFWQNLS
S. cerevisiae	YTKHHQTYVNGFN	GFTNHCLFWENLA
D. radiodurans	HTKHHQTYVDNAN	GHANHSMFWQIMG
E. coli	HTKHHQTYVNNAN	GHANHSLFWKGLK
B. burgdorferi	HSKHHNGFVMNLN	GYSNHTLYFRTLR